PHYSICAL REVIEW B **75**, 094414 (2007)

Edge singularities in high-energy spectra of gapped one-dimensional magnets in strong magnetic fields

A. Friedrich,[1] A. K. Kolezhuk,[2,3] I. P. McCulloch,[1] and U. Schollwöck[1]
[1]*Institut für Theoretische Physik C, RWTH Aachen, 52056 Aachen, Germany*
[2]*Institut für Theoretische Physik, Universität Hannover, 30167 Hannover, Germany*
[3]*Physics Department, Harvard University, 17 Oxford Street, Cambridge, Massachusetts 02138, USA*
(Received 12 December 2006; published 13 March 2007)

We use the dynamical density matrix renormalization group technique to show that the high-energy part of the spectrum of an $S=1$ Heisenberg chain, placed in a strong external magnetic field H exceeding the Haldane gap Δ, contains edge singularities, similar to those known to exist in the low-energy spectral response. It is demonstrated that in the frequency range $\omega \gtrsim \Delta$ the longitudinal (with respect to the applied field) dynamical structure factor is dominated by the power-law singularity $S^{\parallel}(q=\pi,\omega) \propto (\omega-\omega_0)^{-\alpha'}$. We study the behavior of the high-energy edge exponent α' and the edge ω_0 as functions of the magnetic field. The existence of edge singularities at high energies is directly related to the Tomonaga-Luttinger liquid character of the ground state at $H>\Delta$ and is expected to be a general feature of one-dimensional gapped spin systems in high magnetic fields.

DOI: 10.1103/PhysRevB.75.094414 PACS number(s): 75.10.Jm, 75.10.Pq, 75.40.Gb, 75.40.Mg

I. INTRODUCTION

Studying the spectral response is a valuable tool to reveal the properties of the strongly correlated ground state in interacting electronic systems. One of the paradigmatic concepts in physics of one-dimensional (1D) systems is the so-called Tomonaga-Luttinger liquid (TLL),[1] which for 1D systems plays a similar role as does Fermi liquid theory for higher dimensions. One of the prominent features of the TLL is the absence of a quasiparticle peak in the spectral function; instead, there is a power-law singularity, with a nonuniversal exponent that depends on the interaction strength.[2,3]

Apart from 1D conductors (e.g., such as carbon nanotubes[4,5]) and edge states in fractional quantum Hall systems,[6,7] the TLL ground state is expected to exist in several other 1D systems, particularly in spin chains and ladders. For an antiferromagnetic (AF) $S=\frac{1}{2}$ Heisenberg chain, the TLL character of the ground state can be rigorously established from the Bethe ansatz solution,[8] and it is believed[9,10] that this picture is valid also for the other gapless AF chains with half-odd-integer S.

For AF Heisenberg chains with integer S and for spin ladders, which have a finite excitation gap Δ, it has been argued by analytical[11,12] and numerical[13,14] methods that in an external magnetic field $H>\Delta$, strong enough to close the spin gap and cause a finite magnetization, the ground state is also of the TLL type.

Recently, in a search for Luttinger liquid signatures in spin systems, several experimental studies have been undertaken.[15–19] Most of the experimental evidence is, however, indirect, based, e.g., on the analysis of the temperature dependence of specific heat[17,19] or NMR relaxation rate.[18] Direct detection of the low-energy excitation continuum in inelastic neutron scattering experiments[15,16] is a difficult task, not to mention extracting the dynamical exponents from the low-energy spectrum. High-energy modes might be easier to study, especially with techniques such as electron spin resonance.[20,21]

At the same time, the high-energy excitations can be viewed as mobile impurities interacting strongly with the underlying TL liquid, and their spectrum can bear similar features as those found in TLL, namely, the absence of the quasiparticle peak which is replaced by an edge singularity.[22–25] It was shown[23] that the spectrum of high-energy excitations with $S^z=0,1$ contains an edge singularity with a nontrivial field dependence of the edge frequency which in the idealized model with no interaction except the hard-core constraint is given by $\omega_0=(1-S^z)H$. The spectral function of a mobile impurity in the TL liquid has been extensively studied theoretically;[26,27] however, to our knowledge, no numerical results are available to compare with the theoretical predictions. An alternative bosonization description including high-energy modes has been proposed recently.[28] All of this motivates further study of the high-energy spectra of 1D gapped spin systems in strong field.

In the present paper, we study the $S=1$ Heisenberg chain, which is a paradigmatic example of a 1D gapped antiferromagnet. There is a large body of numerical and theoretical results concerning its low-energy behavior in strong fields[12–14,29] which can be used for consistency checks. Using the dynamical density matrix renormalization group (DMRG) technique, we will show that the high-energy part of the spectrum of an $S=1$ chain, placed in a strong external magnetic field H exceeding the Haldane gap Δ, contains edge singularities, similar to the well-known infrared singularities in the low-energy spectral response. It will be demonstrated that in the frequency range $\omega \gtrsim \Delta$ the longitudinal dynamical structure factor is dominated by the continuum with a power-law edge singularity $S^{\parallel}(q=\pi,\omega) \propto (\omega-\omega_0)^{-\alpha'}$. The edge exponent α' is found to decrease as a function of magnetization, and the edge ω_0 is shown to follow approximately the linear law $\omega_0 \simeq H$ as found earlier.[22–24]

II. THEORETICAL PRELIMINARIES

Consider the $S=1$ Heisenberg chain in an applied field described by the Hamiltonian

$$\hat{\mathcal{H}} = J\sum_n \mathbf{S}_n \cdot \mathbf{S}_{n+1} - H\sum_n S_n^z, \tag{1}$$

where $\mathbf{S}_n$ is the spin-1 operator at site n, the exchange constant J will be set to unity, and the external magnetic field H is applied along the z axis. In absence of an applied field, the ground state of the model is a singlet, and the lowest excitations are the triplet of Haldane magnons separated from the ground state by the gap $\Delta \simeq 0.41$ at the wave vector $q=\pi$. The gap closes for $H>H_c=\Delta$, and the system acquires a finite density of $S^z=+1$ magnons, which can be viewed as bosonic particles satisfying the hard-core constraint. It is convenient to redefine the momentum so that the minimum of the magnon dispersion will correspond to zero. Interacting $S^z=1$ magnons form a TL liquid with the Hamiltonian given by

$$\mathcal{H}_0 = \frac{v_F}{2}\int dx\left(\frac{1}{K}(\partial_x\varphi)^2 + K(\partial_x\theta)^2\right), \tag{2}$$

where φ and θ is a pair of bosonic fields satisfying the commutation relations $[\varphi(x),\theta(x')]=i\Theta(x'-x)$ [here $\Theta(x)$ is the Heaviside function] and connected by the duality relation $\partial_t\varphi=v_F\partial_x\theta$. The physical properties of the TL liquid are completely characterized by its Fermi velocity v_F and the TLL parameter K. Both v_F and K are functions of H, and their behavior for the Haldane chain has been studied analytically[12,29] as well as numerically.[13,14] An important feature of the effective TLL description of the Haldane chain is the fact that the parameter K is always larger than unity ($K\to 1$ as $H\to H_c$).

The local spin density $\rho(x)$ (i.e., the density of the sea particles) can be expressed as

$$\rho = S^z = m + \frac{1}{\sqrt{\pi}}\partial_x\varphi + \text{const}\times\sin(2k_Fx + \sqrt{4\pi}\varphi), \tag{3}$$

where $m=m(H)\equiv k_F/\pi$ is the equilibrium magnetization density at the given field. The operator $a^\dagger \sim e^{i\sqrt{\pi}\theta}$ creates a kink in the φ field, shifting it by $\sqrt{\pi}$, and thus corresponds to the creation of an $S^z=1$ particle, so that at low energies one can establish the correspondence $S^+\sim a^\dagger$. The low-energy contribution to the transversal dynamical structure factor (DSF) is thus given by $S^{+-}(q=\pi,\omega) \propto \int dx\int dt\, e^{i\omega t}\langle a^\dagger(x,t)a(0,0)\rangle$, and, since

$$\langle a^\dagger(x,t)a(0,0)\rangle \propto (v_F^2t^2 - x^2)^{-\eta/2} \quad \text{with } \eta = \frac{1}{2K},$$

one readily obtains the infrared singularity

$$S^{+-}(q=\pi,\omega) \propto \frac{1}{\omega^\alpha}, \quad \alpha = 2-\eta, \tag{4}$$

with the edge exponent α determined solely by the TL liquid parameter K.

To describe the excitation of "impurity" particles corresponding to the higher-energy magnon branch with $S^z=0$, one can introduce another bosonic field $b(x)$ described by the Hamiltonian

$$\mathcal{H}_b = \int dx\left(\omega_0 b^\dagger b + \frac{1}{2M}(\partial_x b^\dagger)(\partial_x b)\right). \tag{5}$$

The scaling dimension of the field b is $\dim(b)=\frac{1}{2}$. The TLL action is Lorentz-invariant and thus dictates the dynamical exponent $z=1$, from which one can see that the scaling dimension of the mass M is equal to +1, i.e., M flows to infinity so that one can neglect the impurity dispersion described by the second term in (5); this argument is essentially identical to the dynamical localization of a hole moving in an antiferromagnet as discussed in Ref. 30.

We will be interested in the contribution of the excited impurity particles (b particles) to the dynamical structure factor $S^{zz}(q=\pi,\omega)$, which will be determined by b particles with zero momentum. The local interaction between the impurity particles and the sea particles (a particles) is proportional to the product of the corresponding densities $b^\dagger b\rho$.[31] This yields, apart from renormalizing the energy $\omega_0\mapsto\omega_0 + \text{const}\times m$, two interaction terms: one corresponds to forward scattering and is given by

$$\mathcal{H}_{int}^f = U_f\int dx\frac{1}{\sqrt{\pi}}(\partial_x\varphi)b^\dagger b, \tag{6}$$

and the other, which is proportional to $b^\dagger b\sin(2k_Fx + \sqrt{4\pi}\varphi)$, describes backscattering. The backscattering term, however, is irrelevant since its scaling dimension is $1+K$, and for the Haldane chain one always has $K>1$. With the remaining interaction (6), the Hamiltonian can be diagonalized by means of a unitary transformation[32]

$$\hat{U} = \exp\left(-i\delta\int dx\ \theta(x)b^\dagger(x)b(x)\right) \quad \text{with } \delta = \frac{KU_f}{v_F\sqrt{\pi}}, \tag{7}$$

which changes the phase of the b operator according to

$$b \mapsto \bar{b} = \hat{U}^\dagger b\hat{U} = be^{-i\delta\theta}. \tag{8}$$

Apart from removing the interaction (6), the unitary transformation (7) just renormalizes the threshold energy ω_0, which thus can in principle depend both on the interaction and on the applied field.

Exciting a b particle requires "disturbing" the sea of a particles, because the hard-core constraint leads to a change in the allowed momentum values when the total number of particles is changed.[23] To take the hard-core nature of the bosons into account, we can postulate that the physical creation operator of the b boson can be represented as

$$\psi_b^\dagger = b^\dagger a^\dagger = \bar{b}^\dagger e^{i(\sqrt{\pi}-\delta)\theta}. \tag{9}$$

With that definition, b is the color-changing operator for an existing sea particle, and in the absence of any other interaction except the hard-core constraint the excitation of a b particle would be equivalent to adding another sea boson and the only difference would be the additional energy cost ω_0.

We are interested in the correlator $\langle\psi_b^\dagger(x,t)\psi_b(0,0)\rangle$ because it determines the impurity contribution to the longitudinal DSF:

$$S^{zz}(\pi,\omega) \propto \int dx \int dt\, e^{i\omega t}\langle \psi_b^\dagger(x,t)\psi_b(0,0)\rangle. \qquad (10)$$

Since the $\bar{b}$ quasiparticles are free after the transformation, the correlator factorizes. One has $\langle \bar{b}^\dagger(x,t)\bar{b}(0,0)\rangle \propto \delta(x)e^{-i\omega_0 t}$, where the Dirac δ function $\delta(x)$ is the consequence of irrelevance of the dispersion term in (5), so that

$$\langle \psi_b^\dagger(x,t)\psi_b(0,0)\rangle \propto e^{-i\omega_0 t}\delta(x)/t^{\eta'}, \qquad (11)$$

where

$$\eta' = \frac{1}{2K}\left(1-\frac{KU_f}{\pi v_F}\right)^2 \qquad (12)$$

is the impurity exponent. The longitudinal dynamical structure factor thus contains an edge singularity

$$S^{zz}(\pi,\omega) \propto \frac{1}{(\omega-\omega_0)^{\alpha'}} \quad \text{with } \alpha' = 1-\eta'. \qquad (13)$$

The edge exponent α', in contrast to the low-energy edge exponent α, depends not only on the TL liquid parameter K, but also on the Fermi velocity v_F and on the host-impurity interaction U_f. In the noninteracting hard-core case, which corresponds to $U_f=0$ and $K=1$, this exponent takes the value $\alpha'=\frac{1}{2}$, in agreement with earlier studies.[22–24]

Comparing (13) and (4), one can see that the high-energy DSF exponent $\alpha'=1-\eta'$ should be considerably smaller than the low-energy one $\alpha=2-\eta$. In our approach, this is a direct consequence of the dynamical localization of the impurity, which in turn followed from the nonrelativistic form of the $\mathcal{H}_b$ Hamiltonian (5). It is worthwhile to note that the same answer is obtained by assuming that $\mathcal{H}_b$ has a Lorentz-invariant form and describes a massive field with mass ω_0 and characteristic limiting velocity c. In this latter case $\langle \bar{b}^\dagger(x,t)\bar{b}(0,0)\rangle \propto K_0(\omega_0 r/c)$, where K_0 is the Bessel function, and $r=\sqrt{x^2-c^2t^2}$, and one can show[24] that the corresponding Fourier transform yields the same asymptotic behavior (13).

III. TECHNIQUE

We use the density matrix renormalization group method[33,34] to calculate the spectral function defined earlier. The DMRG works by truncating the Hilbert space of the system, based on selecting the optimal states from the Schmidt decomposition of the lattice as split into two (left and right) blocks. The method we use is a matrix product generalization of the "correction vector method,"[35] in which we calculate the Green's function

$$G(q,\omega+i\delta) = \langle 0|\hat{A}_q^\dagger \frac{1}{E_0+\omega+i\delta-\hat{H}}\hat{A}_q|0\rangle \qquad (14)$$

at a given frequency ω with E_0 being the ground-state energy of the system and δ a numerical broadening, via the so-called correction vector

$$|c(w+i\delta)\rangle = (E_0+w+i\delta-\hat{H})^{-1}\hat{A}_q|0\rangle, \qquad (15)$$

which is determined by a standard linear solver (we used GMRES, but the biconjugate gradient solver is also popular). In contrast to the traditional dynamical DMRG approach where the ground state $|0\rangle$, Lanczos vector $\hat{A}_q|0\rangle$, and correction vector are all determined simultaneously, the matrix product formulation allows the calculation to be split up, improving both the speed and accuracy (for a given size of the truncated Hilbert space) of the calculation. We first calculate the matrix product approximation to the ground state $|0\rangle$ by a standard DMRG calculation, so that we can apply $\hat{A}_q$ exactly to give the Lanczos vector, which is independent of frequency. This is used as input to the correction vector solver which is trivially parallelizable over different frequencies, but we can also, e.g., use a previously determined correction vector from a nearby frequency as the initial guess vector, additionally accelerating the calculation. The matrix product formulation provides good control over the errors, as the residual norm $\|\hat{A}_q|0\rangle-(E_0+w+i\delta-\hat{H})|c(w+i\delta)\rangle\|$ can be calculated exactly. This is prohibitively difficult in the standard DMRG approach as it requires calculating the matrix elements of $\hat{H}^2$ and the usual dynamical DMRG approximation $\hat{H}^2 \simeq (P\hat{H}P^\dagger)^2$, where P is the projector onto the truncated Hilbert space, is inadequate and produces an estimate for the residual norm that is many orders of magnitude too small. Details of this calculation will be provided elsewhere (see also Ref. 36 for a similar approach to this calculation). Given the correction vector, the Green's function can be obtained via

$$G(q,\omega+i\delta) = \langle \hat{A}_q^\dagger|c(\omega+i\delta)\rangle, \qquad (16)$$

from which the spectral function

$$S(q,\omega) = -\frac{1}{\pi}\lim_{\delta\to 0^+} \mathrm{Im}\, G(q,\omega) \qquad (17)$$

can be obtained.

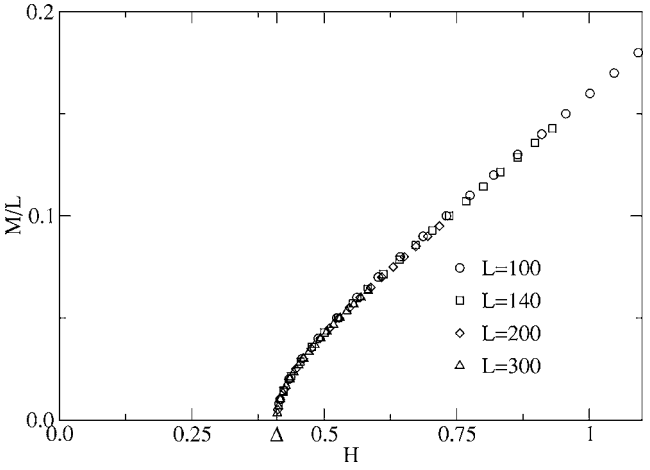

FIG. 1. Ground-state magnetization per site versus magnetic field for different system sizes.

IV. RESULTS AND DISCUSSION

We start with the low-energy properties of the transversal DSF, which are better understood analytically, to show the

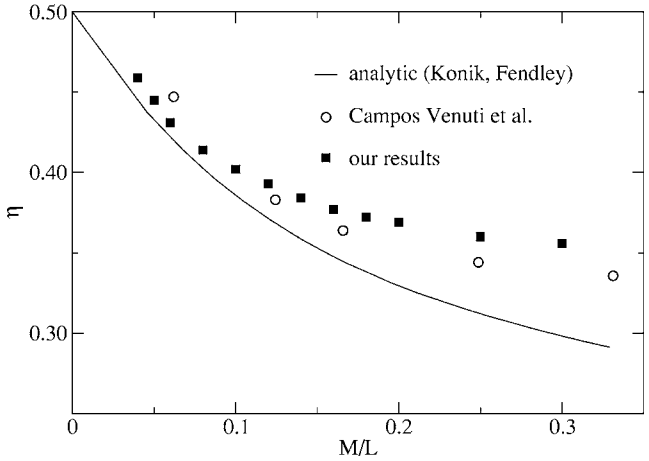

FIG. 2. Exponent η of the static correlation function. Solid line: results obtained from analytic calculations by Konik and Fendley (Ref. 12) based on the effective nonlinear σ-model description. Open circles: DMRG results for short chain lengths $L<80$ obtained by Campos Venuti *et al.* (Ref. 13). Filled squares: our results obtained from DMRG calculations using chains of length $L=200$.

validity of the method. First of all, we have to determine the total spin of the ground state depending on the applied field strength. In Fig. 1 we show the ground-state magnetization M as a function of the magnetic field H; the results for different system sizes are consistent, indicating that finite size effects in $M(H)$ are small for $L \gtrsim 100$.

The exponent η can be obtained from the static transverse spin-spin correlation function $\langle S^x(x)S^x(0)\rangle \sim |x|^{-\eta}$ which is easily accessible in DMRG calculations. From this the TLL parameter can be calculated via $K=1/(2\eta)$. In Fig. 2 we show our values for η and compare them with analytical results based on the effective description in the nonlinear σ-model framework[12] as well as with the earlier DMRG results.[13] From this η we get a first estimate for the edge exponent α via the second equation in Eq. (4).

A typical scan of the low-energy continuum of $S^{+-}(k=\pi,\omega)$ is shown in Fig. 3 for a 200-site chain. The

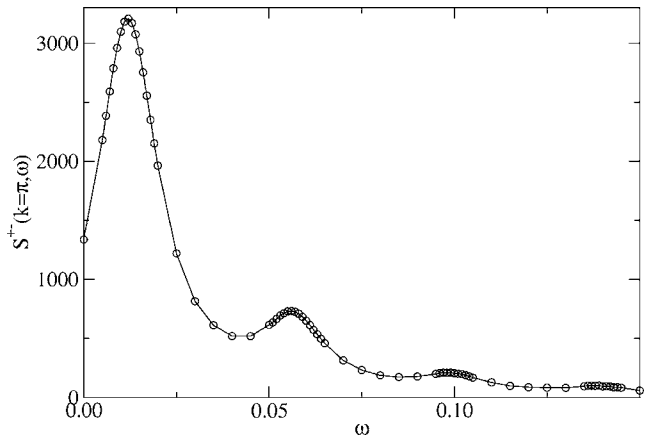

FIG. 3. Spectral function $S^{+-}(k=\pi,\omega)$ for a 200-site chain at magnetic field $H=0.54$ leading to a ground-state magnetization per site of $M/L=0.05$. Here, $\delta=0.01$ and $m=300$ states were kept in the calculation.

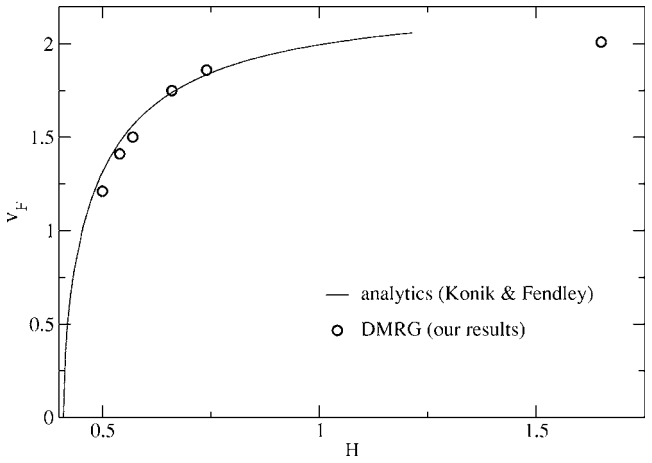

FIG. 4. Fermi velocity extracted from $S^{+-}(k=\pi,\omega)$ as a function of magnetic field (open circles). The solid line corresponds to Eq. (40) of Konik and Fendley (Ref. 12) with the bare spin wave velocity $v_0=2.5$.

magnetic field applied is $H=0.54$ in units of the coupling constant, leading to a ground-state magnetization per site of $M/L=0.05$.

The spectrum reveals a set of peaks at discrete frequency values, as one expects for a finite-size system. The peaks are nearly equidistant (in fact, the distance between the peaks decreases slightly with increasing frequency, which is naturally explained by the effective decrease of the Fermi velocity as the Fermi sea gets emptied by more and more particles being excited). From the energy difference of the first two peaks we extract the Fermi velocity v_F; its dependence on the magnetic field is in good agreement with the results of Konik and Fendley[12] (see Fig. 4) if one sets their parameter v_0 to 2.5. This parameter has the meaning of a bare spin velocity in the nonlinear sigma model description of Konik and Fendley, and the value $v_0 \approx 2.5$ agrees well with the known spin wave velocity $v \approx 2.46$ of the $S=1$ Haldane chain.[37]

One might be tempted to extract the edge exponent α from the dependence of the peak heights in the spectral func-

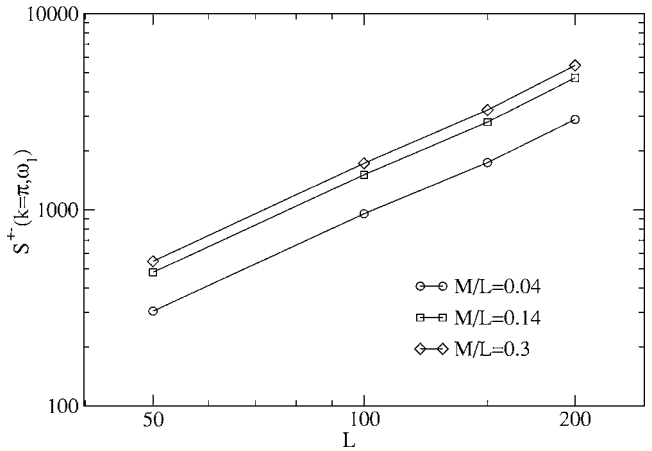

FIG. 5. Peak height of the first peak in $S^{+-}(k=\pi,\omega)$ as a function of the system size L for different magnetizations. Fitting this log-log plot by a straight line yields the edge exponent α.

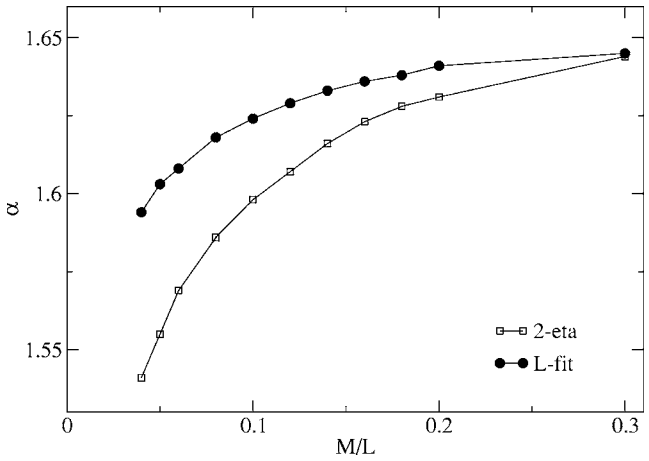

FIG. 6. Edge exponent α obtained from fitting the height of the first peaks in the spectral function versus the chain length by a power law (full circles). The open squares were obtained using Eq. (4).

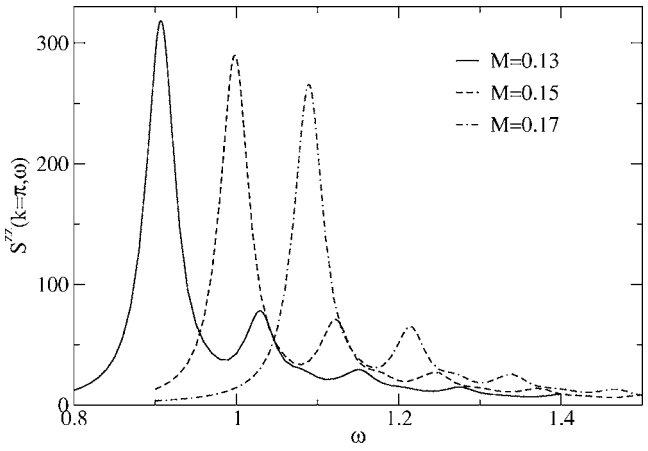

FIG. 7. $S^{zz}(k=\pi,\omega)$ for different magnetizations. Here the numerical broadening is $\delta=0.02$ and $m=500$ states were kept in the reduced DMRG basis.

tion (Fig. 3) on the frequency ω. However, this is not a very good idea: although all these peaks are numerically broadened with the same constant $\delta=0.01$ for an $L=200$-site chain, they do not all show the same width as would have been expected. With increasing frequency they get broader. This can be understood in the following way. The higher the excitation energy is, the more combinations exist to reach it by exciting several particle-hole pairs. In a system with an ideal linear dispersion the energies of all those combinations would be exactly the same and equal $2\pi v_F n/L$ with n being some integer. In a real system the dispersion is not exactly linear, and those energies become slightly scattered around the $2\pi v_F n/L$, contributing an additional broadening to peaks with higher energy. Hence the height of the higher-energy peaks is underestimated and thus the decay is overestimated, leading to a value for the exponent α that is too large.

There is a much better way to determine the edge exponent, namely, from the size dependence of the peak strength. The height of the first peak at ω_1 is given by

$$S^{+-}(k=\pi,\omega_1) \propto 1/\omega_1^{\alpha}.$$

With $\omega_1 \propto v_F/L$ we find

$$S^{+-}(k=\pi,\omega_1) \propto L^{\alpha}$$

for fixed magnetization per site. This is shown in a log-log plot in Fig. 5. From calculations for different chain lengths $L=50,100,150,200$ we find values for α much closer to the expected value.

The values obtained from this L-fit and the expectations from $\alpha=2-\eta$ are compared in Fig. 6. The agreement of both values is good for all M/L (deviation $<5\%$) and gets better for larger magnetizations. Having found a reliable way to extract α we turn to the high-energy continuum in $S^{zz}(k=\pi,\omega)$.

Typical spectra for different magnetizations are shown in Fig. 7. The edge frequency shifts to higher energies with increasing magnetization. Due to the large energy the convergence of the algorithm is worse than for the previous continuum, resulting in a significantly larger DMRG basis. Apart from the expected series of peaks these spectra show small additional peaks between each two peaks. These are finite-size artifacts that vanish for sufficiently large system sizes.

The Fermi velocity extracted from the upper continuum spectra is very similar to the one obtained from the low-energy continuum as shown in Fig. 8.

Like in the low-energy continuum, the peaks get broader with increasing energy, making direct power-law fit of peak intensity vs frequency difficult. Thus, for determining the edge exponent α' the same procedure based on the size dependence is used as in the previous case. From those fits we find the exponent as shown in Fig. 9.

As a further check for the consistency of our data, we show a fit of the high-energy continuum for a magnetization per site $M/L=0.14$ calculated in an $L=100$-site chain. We have fitted the spectrum to a sum of Lorentzians with different widths and with a power-law decay of the peak intensity with the exponent fixed at the value $\alpha'=0.79$ obtained from the analysis of the size dependence of the peak heights. The peak widths and the true edge frequency ω_0 were used as

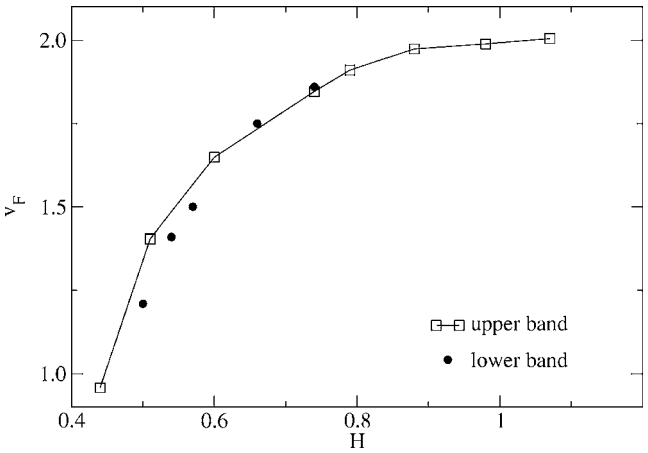

FIG. 8. Fermi velocities extracted from the low-energy spectrum (filled circles) and from the high-energy one (open squares).

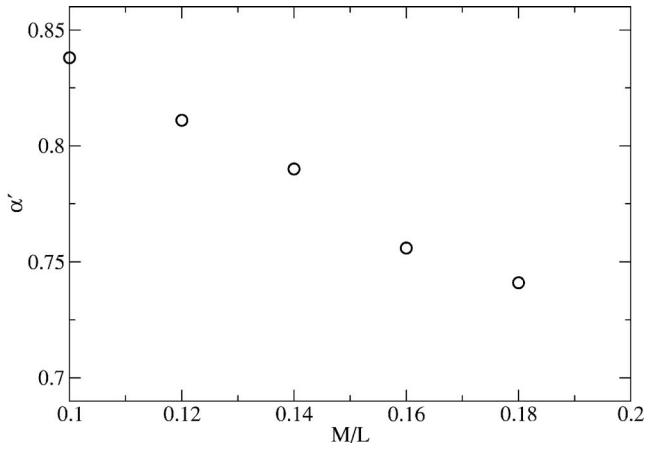

FIG. 9. Edge exponent of the high-energy continuum α' obtained from the L fit of the first peak height for different magnetizations.

fitting parameters. The result is shown in Fig. 10. Since the small shoulder at $\omega \approx 1.13$ is a finite-size effect it has not been fitted. The values obtained for the peak widths γ_i are $\gamma_1=0.0207$, $\gamma_2=0.0236$, $\gamma_3=0.0442$, and $\gamma_4=0.0820$. These widths and the independently obtained α' provide an excellent fit. The true edge frequency $\omega_0=0.929$ is slightly smaller than the position of the first peak $\omega_1=0.952$. To check the validity of this particular value we perform an $L\to\infty$ extrapolation of $\omega_1(L)$ which is supposed to yield the edge frequency. We find $\omega_1(L\to\infty)=0.935$ which is slightly larger than the one found from the fitting procedure.

Notably, the exponent α' decreases with increasing magnetization unlike the edge exponent of the low-energy continuum. With the knowledge of the edge exponent α', the Fermi velocity v_F, and the static exponent η we can extract the effective host-impurity interaction U_f using Eqs. (12) and (13). The values of U_f extracted in that way lie between 7.7 and 8.3, which can be deemed approximately independent of the magnetization (within ±5% accuracy).

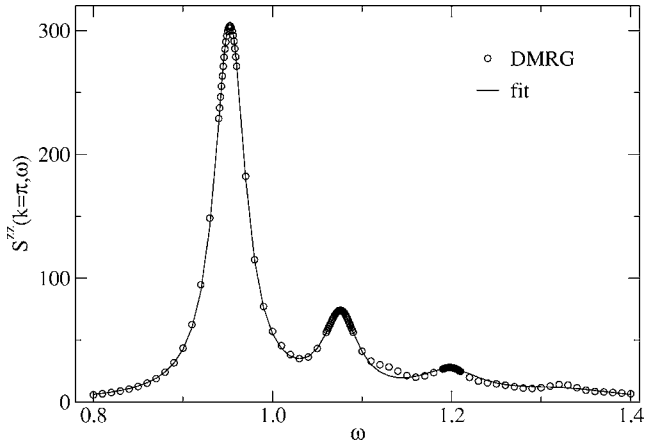

FIG. 10. Circles: $S^{zz}(k=\pi,\omega)$ obtained with $m=500$ states in the DMRG basis. Solid line: Fit by a sum of Lorentzians. For fitting parameters see text.

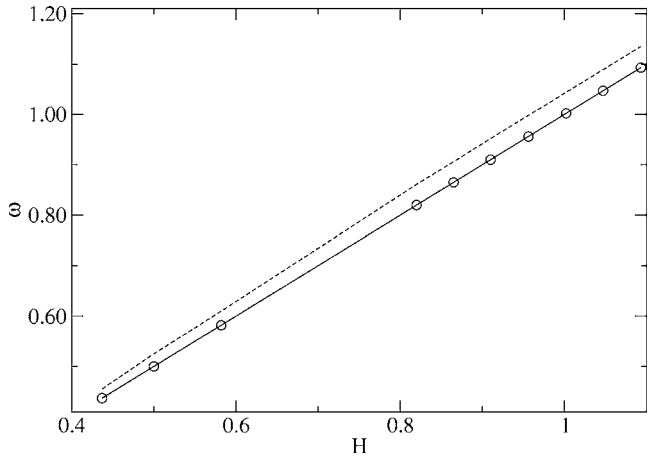

FIG. 11. Position of the first peak as function of the magnetic field (circles). The dashed line denotes $\omega_0=H$ as expected for the idealized hard-core boson model (Refs. 22 and 23).

The position of the first peak ω_1 (which serves as a crude approximation for the true edge frequency ω_0) as a function of the magnetic field shows a clear linear dependence (see Fig. 11). It should be noted that a linear dependence $\omega_0=H$ has been obtained in the idealized hard-core bosonic model,[22,23] as well as in a bosonization calculation[24] for an $S=\frac{1}{2}$ ladder. The observed dependence is quite close to $\omega_0=H$ as seen in Fig. 11.

V. SUMMARY

We have shown that the high-energy spectrum of an $S=1$ Heisenberg chain in a strong external magnetic field H exceeding the Haldane gap Δ contains edge singularities, similar to those known to exist in the low-energy spectral response. It is found that in the frequency range $\omega \gtrsim \Delta$ the longitudinal (with respect to the applied field) dynamical structure factor is dominated by the power-law singularity $S^{\parallel}(q=\pi,\omega)\propto(\omega-\omega_0)^{-\alpha'}$. It is shown that the edge exponent of the high-energy continuum α' decreases with increasing magnetic field, consistent with theoretical expectations. The edge frequency ω_0 is found to increase linearly with the magnetic field, $\omega_0 \simeq cH$, the coefficient c being close to 1, which agrees well with the predictions of Refs. 22–24. The existence of power-law continua with edge singularities at high energies should be a quite general feature, common for all one-dimensional gapped spin systems in high magnetic fields, and directly related to the Tomonaga-Luttinger liquid character of the ground state at $H>\Delta$.

ACKNOWLEDGMENTS

We thank H.-J. Mikeska for fruitful discussions which initiated the present study. A.F. and U.S. acknowledge support by the Deutsche Forschungsgemeinschaft (DFG) under Project No. DFG-Scho 621/4-1. A. K. is supported by the Grant No. KO 2335/1-1 under the Heisenberg Program of the DFG.

[1] S. Tomonaga, Prog. Theor. Phys. **5**, 544 (1950); J. M. Luttinger, J. Math. Phys. **4**, 1154 (1963).
[2] S. Sachdev, T. Senthil, and R. Shankar, Phys. Rev. B **50**, 258 (1994).
[3] H. J. Schulz, Phys. Rev. B **34**, 6372 (1986).
[4] M. Bockrath, D. H. Cobden, J. Lu, A. G. Rinzler, R. E. Smalley, L. Balents, and P. L. McEuen, Nature (London) **397**, 598 (1999); R. Egger, A. Bachtold, M. S. Fuhrer, M. Bockrath, D. H. Cobden, and P. L. McEuen, in *Interacting Electrons in Nanostructures*, edited by R. Haug and H. Schoeller, Lecture Notes in Physics Vol. 579 (Springer-Verlag, Berlin, 2001), p. 125.
[5] H. Ishii, H. Kataura, H. Shiozawa, H. Yoshioka, H. Otsubo, Y. Takayama, T. Miyahara, S. Suzuki, Y. Achiba, M. Nakatake, T. Narimura, M. Higashiguchi, K. Shimada, H. Namatame, and M. Taniguchi, Nature (London) **426**, 540 (2003).
[6] X. G. Wen, Phys. Rev. B **41**, 12838 (1990).
[7] M. Stone, Phys. Rev. B **42**, 8399 (1990).
[8] F. D. M. Haldane, Phys. Rev. Lett. **45**, 1358 (1980).
[9] F. D. M. Haldane, Phys. Rev. Lett. **50**, 1153 (1983).
[10] I. Affleck and F. D. M. Haldane, Phys. Rev. B **36**, 5291 (1987).
[11] R. Chitra and T. Giamarchi, Phys. Rev. B **55**, 5816 (1997).
[12] R. M. Konik and P. Fendley, Phys. Rev. B **66**, 144416 (2002).
[13] L. Campos Venuti, E. Ercolessi, G. Morandi, P. Pieri, and M. Roncaglia, Int. J. Mod. Phys. B **16**, 1363 (2002).
[14] G. Fath, Phys. Rev. B **68**, 134445 (2003).
[15] L.-P. Regnault, A. Zheludev, M. Hagiwara, and A. Stunault, Phys. Rev. B **73**, 174431 (2006).
[16] M. Hagiwara, L. P. Regnault, A. Zheludev, A. Stunault, N. Metoki, T. Suzuki, S. Suga, K. Kakurai, Y. Koike, P. Vorderwisch, and J.-H. Chung, Phys. Rev. Lett. **94**, 177202 (2005).
[17] M. Hagiwara, H. Tsujii, C. R. Rotundu, B. Andraka, Y. Takano, N. Tateiwa, T. C. Kobayashi, T. Suzuki, and S. Suga, Phys. Rev. Lett. **96**, 147203 (2006).
[18] K. Izumi, T. Goto, Y. Hosokoshi, and J.-P. Boucher, Physica B **329-333**, 1191 (2003).
[19] Y. Yoshida, N. Tateiwa, M. Mito, T. Kawae, K. Takeda, Y. Hosokoshi, and K. Inoue, Phys. Rev. Lett. **94**, 037203 (2005).
[20] M. Orendáč, S. Zvyagin, A. Orendáčová, M. Seiling, B. Lüthi, A. Feher, and M. W. Meisel, Phys. Rev. B **60**, 4170 (1999).
[21] M. Hagiwara, Z. Honda, K. Katsumata, A. K. Kolezhuk, and H.-J. Mikeska, Phys. Rev. Lett. **91**, 177601 (2003).
[22] A. K. Kolezhuk and H.-J. Mikeska, Prog. Theor. Phys. Suppl. **145**, 85 (2002).
[23] A. K. Kolezhuk and H.-J. Mikeska, Phys. Rev. B **65**, 014413 (2002).
[24] A. Furusaki and S.-C. Zhang, Phys. Rev. B **60**, 1175 (1999).
[25] S. Sorella and A. Parola, Phys. Rev. Lett. **76**, 4604 (1996).
[26] A. H. Castro Neto and M. P. A. Fisher, Phys. Rev. B **53**, 9713 (1996).
[27] Y. Tsukamoto, T. Fujii, and N. Kawakami, Phys. Rev. B **58**, 3633 (1998).
[28] M. Sato, J. Stat. Mech., P09001 (2006).
[29] I. Affleck, cond-mat/0508354 (unpublished).
[30] S. Sachdev, M. Troyer, and M. Vojta, Phys. Rev. Lett. **86**, 2617 (2001).
[31] Here we are interested only in the dynamical structure factor at the wave vector $q=\pi$ which corresponds to the impurity with zero momentum. In the case of nonzero momentum an additional term of the type $iV_f^a \int dx[b^\dagger \partial_x b - (\partial_x b^\dagger) b](\partial_x \theta)$, which is a product of currents corresponding to a and b particles, could be present in the forward scattering (Ref. 27). This term can be dealt with in a similar way [Ref. 27; G. A. Fiete, Phys. Rev. Lett. **97**, 256403 (2006)] leading to a wave-vector-dependent edge exponent.
[32] I. Affleck and A. W. W. Ludwig, J. Phys. A **27**, 5375 (1994).
[33] S. R. White, Phys. Rev. Lett. **69**, 2863 (1992).
[34] U. Schollwöck, Rev. Mod. Phys. **77**, 259 (2005).
[35] T. D. Kühner and S. R. White, Phys. Rev. B **60**, 335 (1999).
[36] F. Verstraete, A. Weichselbaum, U. Schollwöck, J. I. Cirac, and Jan von Delft, cond-mat/0504305 (unpublished).
[37] S. R. White, Phys. Rev. Lett. **69**, 2863 (1992).